



# Synchronization of phase oscillators with coupling mediated by a diffusing substance

C.A.S. Batista<sup>a</sup>, J.D. Szezech Jr.<sup>b</sup>, A.M. Batista<sup>b</sup>, E.E.N. Macau<sup>c</sup>, R.L. Viana<sup>d,\*</sup>

<sup>a</sup> Center for Marine Studies, Federal University of Paraná, Pontal do Paraná, Paraná, Brazil

<sup>b</sup> Department of Mathematics and Statistics, State University of Ponta Grossa, Ponta Grossa, Paraná, Brazil

<sup>c</sup> National Institute of Space Research, São José dos Campos, São Paulo, Brazil

<sup>d</sup> Department of Physics, Federal University of Paraná, Curitiba, Paraná, Brazil

## HIGHLIGHTS

- When phase oscillators produce and absorb a diffusing substance non-local couplings are produced.
- The nonlocal coupling has an exponential decay in the one-dimensional case.
- There is a transition to phase and frequency synchronization as the coupling parameters are varied.

## ARTICLE INFO

### Article history:

Received 24 November 2016

Available online 7 December 2016

### Keywords:

Synchronization

Phase oscillators

Nonlocal coupling

## ABSTRACT

We investigate the transition to phase and frequency synchronization in a one-dimensional chain of phase oscillator “cells” where the coupling is mediated by the local concentration of a chemical which can diffuse in the inter-oscillator medium and it is both secreted and absorbed by the oscillator “cells”, influencing their dynamical behavior. This coupling has the advantage of having a tunable parameter which makes it possible to pass continuously from a global (all-to-all) to a local (nearest-neighbor) coupling form. We have verified that synchronous behavior depends on the coupling strength and coupling length.

© 2016 Elsevier B.V. All rights reserved.

## 1. Introduction

In many problems of physical and biological interest nonlinear oscillators (or “cells”) have been considered, whose interaction is mediated through a chemical substance which is secreted by the cells and diffuses along the intercellular medium, being absorbed by the cells [1]. Moreover, the rate of secretion depends on the cell dynamics, as well as the rate of absorption. In this way the dynamics of the cells are effectively coupled by the diffusing chemical substance, leading to a non-local coupling type which depends on the details of the diffusion process.

This kind of chemical coupling can be mathematically described by a model proposed by Kuramoto leading to non-local couplings [2–4]. In this model the state variables of each oscillator influence the secretion of a chemical substance obeying a diffusion equation. The rate of absorption depends on the local concentration of this substance at each cell position [5–9].

The non-local coupling obtained in this way has an exponentially decreasing dependence on the spatial position and depends on a parameter, the inverse coupling length, which can take one any real value from zero to infinity. These are the limits when the coupling becomes global (all-to-all) and local (nearest-neighbor), respectively. A similar coupling is based

\* Corresponding author.

E-mail address: [viana@fisica.ufpr.br](mailto:viana@fisica.ufpr.br) (R.L. Viana).

on a power-law instead of an exponential type, but does not have a direct interpretation in terms of a diffusing chemical in the intercell medium [10–12].

Global coupling of oscillators has been intensively studied both numerically and analytically, particularly for the Kuramoto model of phase oscillators, for which it is possible to use a mean-field theory to describe the collective behavior of the assembly [13,14]. In this model the phase oscillators have natural frequencies, randomly distributed according to a given probability function. If the coupling strength is too weak the coupling effect is not strong enough to overcome the original disorder of the system and the phases remain uncorrelated.

For a coupling strength higher than a critical value, though, some of the oscillators begin to synchronize their frequencies, while their phases become locked to each other. By defining a suitable order parameter it is possible to describe the transition from a non-synchronized to a (partially) synchronized state by means of a continuous phase transition. Many efforts have been made to extend some of these results to other kinds of complex networks [15–17].

In this work we present results of numerical simulations of Kuramoto-type phase oscillators which are coupled according to a chemical coupling, in which the strength decreases exponentially with the lattice distance for a one-dimensional chain. We treat separately phase and frequency synchronization, using different numerical diagnostics for them, and investigating the occurrence of the transition between non-synchronized and partially synchronized states. The coupling parameters considered here were the strength and the inverse coupling length, which can vary continuously so as to simulate chains with local or non-local couplings.

This paper is organized as follows: in Section 2 we describe the coupling model based on the diffusion of a chemical which is both secreted and absorbed by the oscillators, so affecting their dynamics (chemical coupling). We also show how to obtain Kuramoto-like models in a one-dimensional chain (with periodic boundary conditions) from this general framework. Section 3, which deals with frequency synchronization, introduces appropriate diagnostics of synchronization and uses them to evidence transitions. A similar treatment is applied in Section 4 for phase synchronization. In Section 5 we use a characterization for spatial complexity using a recurrence-based technique. The last section is devoted to our conclusions.

## 2. Coupling model

In the following we will deal with two classes of vectors, which are represented by a different notation: (i) positions  $\vec{r}$  in a  $d$ -dimensional Euclidean space, to which the oscillators belong; (ii) state variables  $\mathbf{X} = (x_1, x_2, \dots, x_M)^T$  in a  $M$ -dimensional phase space of the dynamical variables characterizing the state of the system at a given time  $t$ . There are  $N$  oscillator cells located at discrete positions  $\vec{r}_j$ , where  $j = 1, 2, \dots, N$ , in the  $d$ -dimensional Euclidean space; and  $\mathbf{X}_j$  is the state variable for each oscillator, whose time evolution is governed by the vector field  $\mathbf{F}(\mathbf{X}_j)$  [Fig. 1]. The oscillators are not supposed to be identical, though, for they can have slightly different parameters.

We suppose that the time evolution is affected by the local concentration of a chemical, denoted as  $A(\vec{r}, t)$ , through a time-dependent coupling function  $\mathbf{g}$ :

$$\frac{d\mathbf{X}_j}{dt} = \mathbf{F}(\mathbf{X}_j) + \mathbf{g}(A(\vec{r}_j, t)), \quad (1)$$

whereas the chemical concentration satisfies a diffusion equation of the form

$$\varepsilon \frac{\partial A(\vec{r}, t)}{\partial t} = -\eta A(\vec{r}, t) + D \nabla^2 A(\vec{r}, t) + \sum_{k=1}^N h(\mathbf{X}_k) \delta(\vec{r} - \vec{r}_k), \quad (2)$$

where  $\varepsilon \ll 1$  is a small parameter representing the fact that diffusion occurs in a timescale faster than the intrinsic period of individual oscillators;  $\eta$  is a phenomenological damping parameter (representing the chemical degradation of the mediating substance), and  $D$  is a diffusion coefficient. The diffusion equation above has a source term  $h$  which depends on the oscillator state at the discrete positions  $\vec{r}_j$ ; this means that each oscillator secretes the chemical with a rate depending on the current value of its own state variable.

We assume, as in Ref. [2], that the diffusion is so fast, compared with the oscillator period, that we may set  $\varepsilon \dot{A} = 0$  such that the concentration relaxes to a stationary value that can be written in the following form:

$$A(\vec{r}_j) = \sum_{k=1}^N \sigma(\vec{r}_j - \vec{r}_k) h(\mathbf{X}_k), \quad (3)$$

where  $\sigma(\vec{r}_j - \vec{r}_k)$  is a Green function (also called interaction kernel), which is the solution of

$$(\eta - D \nabla^2) \sigma(\vec{r}_j - \vec{r}) = \delta(\vec{r}_j), \quad (4)$$

such that we have eliminated adiabatically the chemical concentration and, on substituting (3) into Eq. (2) we obtain the general equation expressing chemical coupling in the adiabatic approximation

$$\frac{d\mathbf{X}_j}{dt} = \mathbf{F}(\mathbf{X}_j) + \mathbf{g} \left( \sum_{k=1}^N \sigma(\vec{r}_j - \vec{r}_k) h(\mathbf{X}_k) \right). \quad (5)$$

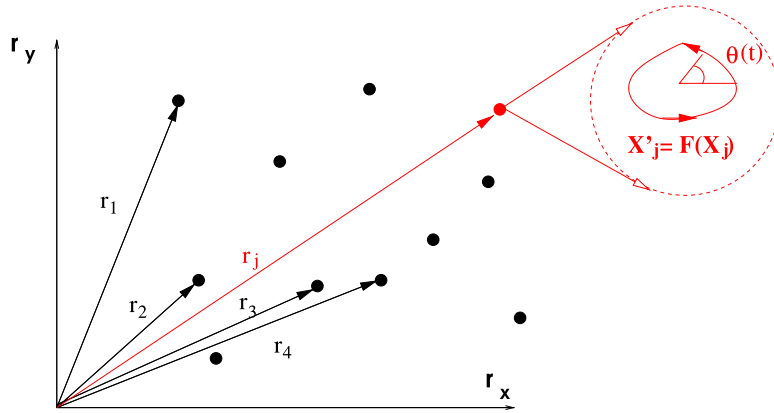


**Fig. 1.** (Color online) Schematic figure of the model for coupling among phase oscillators mediated by a diffusing substance.

If  $\mathbf{g}$  is a linear function of  $\mathbf{X}_j$  (and not of the positions  $\vec{r}_j$ ) we write

$$\frac{d\mathbf{X}_j}{dt} = \mathbf{F}(\mathbf{X}_j) + \sum_{k=1}^N \sigma(\vec{r}_j - \vec{r}_k) \mathbf{g}(h(\mathbf{X}_k)). \quad (6)$$

We are particularly interested in nonlinear couplings, for which

$$\mathbf{g}(h(\mathbf{X}_k)) = \mathbf{A}\mathbf{H}(\mathbf{X}_k), \quad (7)$$

where  $\mathbf{A}$  is a  $M \times M$  matrix indicating which variables of the oscillators are coupled to whom, and  $\mathbf{H}$  is a nonlinear function of its arguments.

In this work we are interested in a case of nonlinear coupling of phase oscillators, for which we take  $M = 1$  such that  $\mathbf{X}_j$  is a geometrical phase  $\theta_j \in [0, 2\pi)$ , and the vector function  $\mathbf{F}(\mathbf{X}_j)$  is the corresponding frequency  $\omega_j$  (different for each oscillator, in general). In this case  $\mathbf{A}$  reduces to a scalar coupling strength  $K$  and the nonlinear coupling function is

$$\mathbf{H}(\mathbf{X}_k) = \sin(\theta_k - \theta_j), \quad (8)$$

yielding a chemically coupled Kuramoto model

$$\dot{\theta}_j = \omega_j + K \sum_{k=1}^N \sigma(\vec{r}_j - \vec{r}_k) \sin(\theta_k - \theta_j). \quad (9)$$

From the Fourier transform of Eq. (4), the interaction kernel can be formally written, when  $d$  is the spatial dimension of the system, as

$$\sigma(\vec{r}_j - \vec{r}) = \frac{1}{(2\pi)^d} \int d^d q \frac{e^{iq \cdot (\vec{r}_j - \vec{r})}}{\eta + D|\vec{q}|^2}. \quad (10)$$

When the system is isotropic, the kernel becomes a function of the distance  $r = |\vec{r}_j - \vec{r}|$ , and can be expressed, in the one-dimensional case, by

$$\sigma(r) = C \exp(-\gamma r), \quad (11)$$

where  $\gamma$  is the inverse of the coupling length, given by

$$\gamma = \sqrt{\frac{\eta}{D}}, \quad (12)$$

and the constant  $C$  is determined from the normalization condition

$$\sum_{j=1}^N \sigma(|\vec{r}_j - \vec{r}|) = 1. \quad (13)$$

A generalized Kuramoto model can be obtained out of the foregoing description by building a one-dimensional lattice of  $N$  (an odd number) fixed and equally spaced phase oscillators with non-local interactions given by the kernel (11) for  $d = 1$ . The generalization to two and three dimensions is straightforward but the need of considering all neighbors of a given oscillator poses a serious obstacle due to the eventually prohibitive computer time required to take into account all interactions. Another possibility (not taken into account in this work) is to consider a random distribution of oscillators

along the lattice. However, if we are interested to study systematically the effect of the lattice distance on the dynamical properties it is interesting to consider a regular lattice. Assuming that the distance between consecutive sites is a constant  $\Delta$ , and supposing periodic boundary conditions

$$\theta_j = \theta_{j \pm N'}, \quad N' = \frac{N-1}{2}, \tag{14}$$

we can write  $|\vec{r}_j - \vec{r}_k| = (j-k)\Delta \equiv \ell\Delta$  by changing the summation index from  $k = 1, 2, \dots, N$  to  $\ell = j-k$ , such that  $\ell = \pm 1, \pm 2, \dots, \pm N'$ . This leaves us with  $2N' + 1 = N$  sites, each of them with a distance  $\ell$  from any site  $j$ . The Green function is thus

$$\sigma(|\vec{r}_j - \vec{r}_\ell|) = Ce^{-\gamma\Delta\ell}. \tag{15}$$

On excluding self-interactions, or the coupling of any site with itself, we replace the sum over  $k$  in Eq. (9) by two sums, one over  $\ell = 1, 2, \dots, N'$  and other over  $\ell = -1, -2, \dots, -N'$ . In the latter sum we can change index again  $m = -\ell$  and then replace  $m$  by  $\ell$  since they are dummy indexes. Hence the first sum considers  $k = j - \ell$  and the second one  $k = j + \ell$ , such that we can group them together into a single summation, yielding

$$\dot{\theta}_j = \omega_j + K \sum_{\ell=1}^{N'} Ce^{-\gamma\Delta\ell} [\sin(\theta_{j-\ell} - \theta_j) + \sin(\theta_{j+\ell} - \theta_j)]. \tag{16}$$

Making the same changes of index we previously did the result is

$$C = \left[ 2 \sum_{\ell=1}^{N'} e^{-\gamma\Delta\ell} \right]^{-1}. \tag{17}$$

The value of  $\Delta$  is immaterial and we will make  $\Delta = 1$  from now on for simplicity. Hence (16) can be rewritten as

$$\dot{\theta}_j = \omega_j + \frac{K}{2 \sum_{\ell=1}^{N'} e^{-\gamma\ell}} \sum_{\ell=1}^{N'} e^{-\gamma\ell} [\sin(\theta_{j-\ell} - \theta_j) + \sin(\theta_{j+\ell} - \theta_j)]. \tag{18}$$

It is interesting to investigate the limiting cases of this form of coupling. If  $\gamma$  goes to zero then,

$$C = \frac{1}{2N'} = \frac{1}{N-1}, \tag{19}$$

and we have a global type of coupling

$$\dot{\theta}_j = \omega_j + \frac{K}{N-1} \sum_{k=1}^N \sin(\theta_k - \theta_j), \tag{20}$$

which is very similar to the classical Kuramoto model of coupled phase oscillators, except for the denominator which is  $N$  instead of  $N - 1$ , as in Eq. (20).

In the limit of  $\gamma$  large, the exponential in the Green function decays very fast with the lattice distance  $\ell$ , such that only the term with  $\ell = 1$  contributes significantly to the summations. This gives, for the normalization constant

$$C \approx \frac{1}{2e^{-\gamma\Delta}} \tag{21}$$

and the coupling term takes into account only the nearest neighbors of a given site

$$\dot{\theta}_j = \omega_j + \frac{K}{2} [\sin(\theta_{j-1} - \theta_j) + \sin(\theta_{j+1} - \theta_j)] \tag{22}$$

which is the usual local (diffusive or Laplacian) coupling. Hence, depending on the value of the inverse coupling length we can pass continuously from a global to a local coupling type. A similar prescription for non-local couplings was proposed by Rogers and Wille, who considered a power-law spatial dependence  $\ell^{-\delta\alpha}$  instead of an exponential decay as here. In spite of the differences, both non-local couplings present similar properties with respect to the synchronized behavior of the oscillator chain.

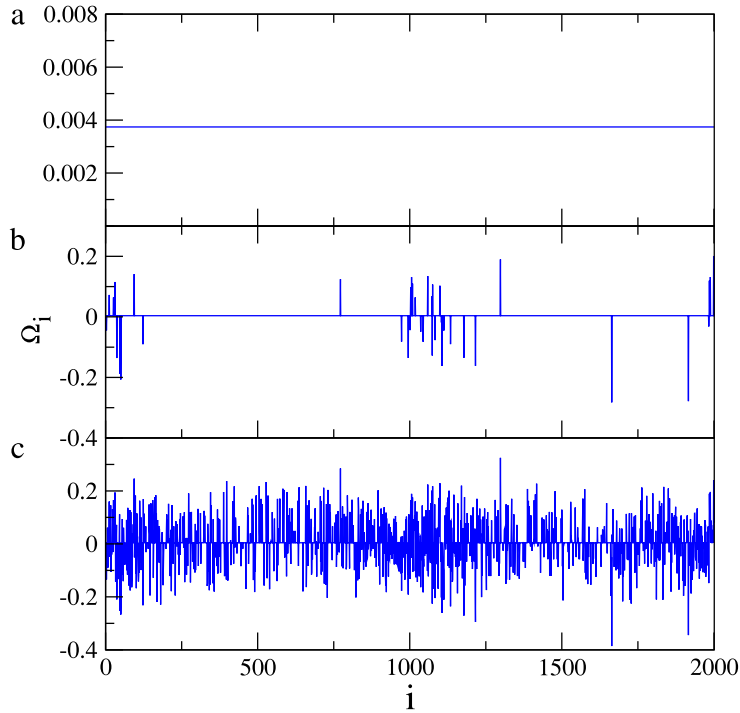


**Fig. 2.** (Color online) Perturbed frequencies of a chain with  $N = 2001$  Kuramoto oscillators at fixed time 15 000, with coupling strength  $K = 7$  and inverse coupling lengths  $\gamma = 0.0030$  (a), 0.0045 (b), and 0.0050 (c).

### 3. Frequency synchronization

Given that  $\theta_j$  is a phase angle for the  $j$ th oscillator we are interested in its phase rate  $\Omega_j = \dot{\theta}_j$ , which can be called perturbed frequency. From (18) it follows that the difference between the latter and the natural frequencies  $\omega_j$  is just the coupling term induced by the diffusing chemical:

$$\Omega_j - \omega_j = \frac{K}{2 \sum_{\ell=1}^{N'} e^{-\gamma \ell}} \sum_{\ell=1}^{N'} e^{-\gamma \ell} [\sin(\theta_{j-\ell} - \theta_j) + \sin(\theta_{j+\ell} - \theta_j)], \quad (23)$$

in such a way that, for uncoupled oscillators ( $K = 0$ )  $\Omega_j = \omega_j$ . We assume that uncoupled oscillators have randomly chosen natural frequencies  $\omega_j$  according to a given probability distribution function  $g(\omega)$ . It is customary to use a unimodal and symmetric PDF such that  $g(-\omega) = g(\omega)$  with a maximum at  $g(0)$ , i.e.  $g'(0) = 0$  and  $g''(0) < 0$ .

We consider that initially the oscillators have randomly distributed phases, i.e. the values of  $\theta_j(t = 0)$  are chosen within the interval  $[0, 2\pi)$  using a uniform probability distribution. The coupled differential equations described by (18) are numerically solved using a fourth-order Runge–Kutta solver for given values of the coupling strength  $K$  and the inverse coupling length  $\gamma$ . At each time, the perturbed frequencies are obtained as

$$\Omega_j = \lim_{t \rightarrow \infty} \frac{\theta_j(t + T) - \theta_j(T)}{t}, \quad (j = 1, 2, \dots, N), \quad (24)$$

where  $T$  is chosen such that transients have decayed.

Two or more phase oscillators are said to be frequency synchronized if their frequencies are equal, up to a specified tolerance. If the oscillators are synchronized in frequency this does not mean necessarily that their phases are equal (phase synchronization). For example, two oscillators which are anti-phase synchronized have nevertheless the same frequencies. However, phase synchronization do imply frequency synchronization.

Let us first consider the case of (relatively) large  $\gamma$  [Fig. 2(c)]: at a fixed time most of the oscillators have different frequencies but some of them are frequency-synchronized. Keeping the coupling strength  $K$  constant and decreasing  $\gamma$  we observe that many oscillators become frequency synchronized at  $\Omega = 0$  [Fig. 2(b)]. This is not surprising, though, as the natural frequencies are distributed around  $\omega = 0$ . Finally, for smaller  $\gamma$  all oscillators in the chain have the same frequencies [Fig. 2(a)]. This shows that the coupling length plays a role on the synchronization properties of the chain.

In Fig. 2(b) we see that, when some oscillators are no longer synchronized, there is a number of synchronization plateaus with different lengths. Let  $N_i$  be the length of the  $i$ th plateau, and  $N_p$  the total number of them, with average size

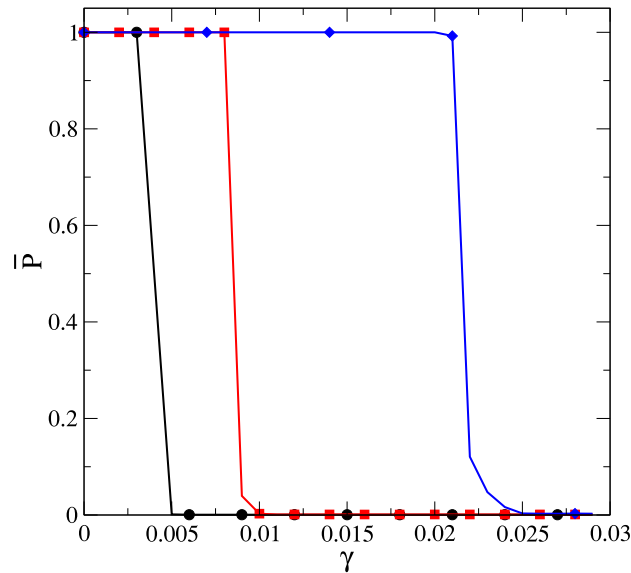


**Fig. 3.** Frequency synchronization degree as a function of the inverse coupling length  $\gamma$  for a chain of  $N = 2001$  Kuramoto oscillators with  $K = 7$  and different lattice sizes:  $N = 401$  (blue line),  $1001$  (red line), and  $2001$  (black line). (For interpretation of the references to color in this figure legend, the reader is referred to the web version of this article.)

$\langle N \rangle = (1/N_p) \sum_{i=1}^{N_p} N_i$ . We define a synchronization degree  $P$  as the ratio between the average plateau length and the total lattice size  $N$ , or  $P = \langle N \rangle / N$ .

For a totally synchronized state, as that depicted in Fig. 2(a), we have just one plateau comprising the entire lattice ( $\langle N \rangle = N$ ) so that  $P = 1$ . On the other hand, for a completely non-synchronized state there are almost as many plateaus as sites, so  $N_p \approx N$ , or  $\langle N \rangle \approx 1$ , giving  $P \approx 1/N \rightarrow 0$ , if  $N \rightarrow \infty$ , as shown in Fig. 2(c). A quantity similar to the synchronization degree is the frequency-order parameter introduced by Sakaguchi et al. [9]:  $E = N_E / N$ , where  $N_E$  is the number of oscillators in the largest plateau.

Fig. 3 illustrates the variation of the average synchronization degree with the inverse coupling length for a fixed coupling strength  $K$  and different lattice sizes. In the three cases depicted a common feature is that, if  $\gamma$  is small enough the oscillators are frequency-synchronized and, as  $\gamma$  increases past a critical value  $\gamma_c$ , there is a transition to a non-synchronized state (or, more properly, to a partially synchronized one). It turns out that  $\gamma_c$  decreases as we increase the lattice size.

By way of contrast, if we keep  $\gamma$  fixed and vary the coupling strength  $K$ , a similar transition to frequency synchronization occurs, after  $K$  increases past a critical value  $K_c$ . As a matter of fact, the occurrence of frequency synchronization depends on both coupling parameters ( $\gamma$  and  $K$ ) as illustrated by Fig. 4, where we depict the region of frequency synchronization (according to the value of the synchronization degree  $P$ ) as a function of  $\gamma$  and  $K$ . The transition to frequency synchronization occurs past a critical line which is indicated by the squares depicted in Fig. 4. Due to the horizontal scale adopted it seems that there is always frequency synchronization for the global case ( $\gamma = 0$ ), which is not the case, as illustrated by the inset of Fig. 4, where we show a magnification of the lower right hand corner. In the latter case the critical coupling strength in the globally coupled case is  $K_c \approx 0.08$ .

Since uncoupled oscillators have randomly distributed natural frequencies, the onset of frequency synchronization appears due to the dominant effect of the coupling over the randomness of the original distribution. For global couplings ( $\gamma = 0$ ) the value of  $K_c$  is close to zero, indicating that a synchronized state occurs for very weak couplings. Local couplings, where  $\gamma$  is large enough, however, may not yield frequency synchronization even if  $K$  is very large. These features are typical of structural phase transitions and are best explained by considering phase synchronization.

#### 4. Phase synchronization

In an oscillator chain, a completely phase-synchronized state is characterized by the equality of the oscillator phases for any times:

$$\theta_1(t) = \theta_2(t) = \dots = \theta_N(t). \quad (25)$$

Clusters of phase-synchronized oscillators are defined in a similar way. A useful diagnostic of phase synchronization is the complex order parameter introduced by Kuramoto [14]

$$z(t) = R(t)e^{i\varphi(t)} = \frac{1}{N} \sum_{j=1}^N e^{i\theta_j(t)}. \quad (26)$$

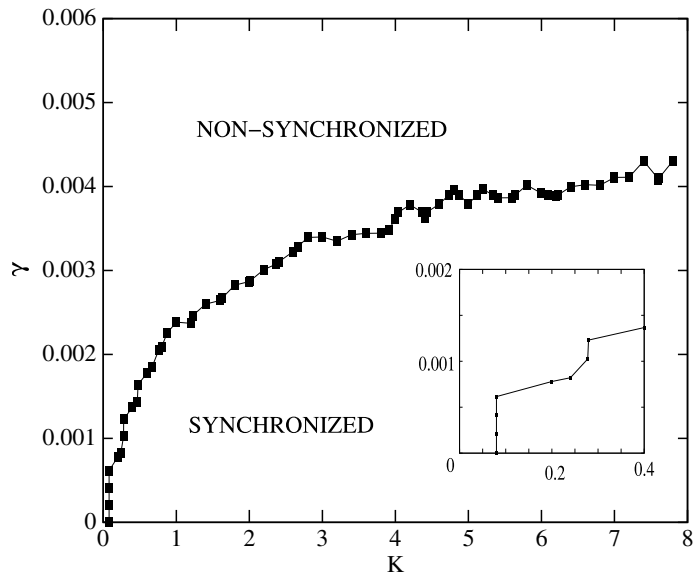


**Fig. 4.** Regions of frequency synchronization, according to the value of the synchronization degree  $P$ , vs. coupling parameters (coupling strength  $K$  and inverse coupling length  $\gamma$ ) for a chain of  $N = 2001$  Kuramoto oscillators. The squares indicate the boundary of the frequency-synchronized region. In the inset we show a magnification of the lower right corner of the figure.

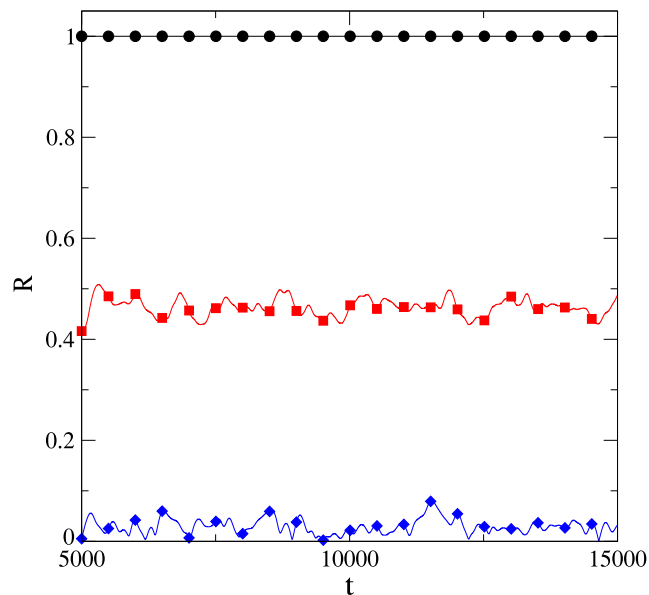


**Fig. 5.** Time evolution of the order parameter magnitude for  $K = 7$  and  $\gamma = 0.001$  (black line),  $0.005$  (red line) and  $0.006$  (blue line) for a chain of  $N = 2001$  Kuramoto oscillators. (For interpretation of the references to color in this figure legend, the reader is referred to the web version of this article.)

The quantities  $R$  and  $\varphi \in [0, 2\pi)$  are respectively the amplitude and angle of a gyrating vector which is equal to the vector sum of phasors for each oscillator in a one-dimensional lattice with periodic boundary conditions. In order to see the meaning of  $z(t)$  let us analyze two limits cases. Firstly, for a completely phase-synchronized state the order parameter magnitude is  $R(t) = 1$  for all times. In the second place, let us consider a completely non-synchronized pattern, for which the phases are so spatially uncorrelated that they can be considered as randomly distributed over  $[0, 2\pi)$ . The order parameter in this case has zero magnitude since it is a space-average over randomly distributed variables. Intermediate values of  $R$  thus represent partially synchronized states.

In Fig. 5 we plot the order parameter magnitude as a function of time for  $K = 7$  and three different values of the inverse coupling length  $\gamma$ . The case  $\gamma = 0.001$  is the most akin to a global coupling, and exhibits a completely phase-synchronized state. Higher values of  $\gamma$  lead to partially synchronized states. For  $\gamma = 0.006$  the parameter  $R$  exhibits small-amplitude fluctuations near zero, indicating a nearly non-synchronized state. Since  $R$  typically fluctuates with time we prefer to work

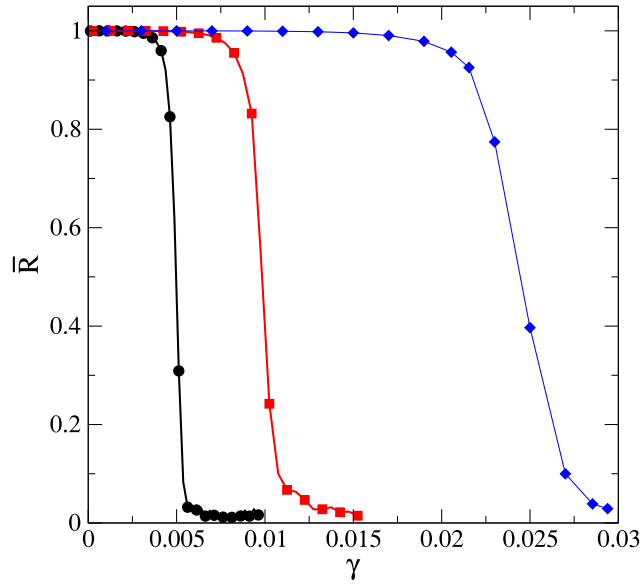


**Fig. 6.** Time-averaged order parameter magnitude versus inverse coupling length  $\gamma$  for  $K = 7$  and different lattice sizes:  $N = 401$  (blue line), 1001 (red line), and 2001 (black line). (For interpretation of the references to color in this figure legend, the reader is referred to the web version of this article.)

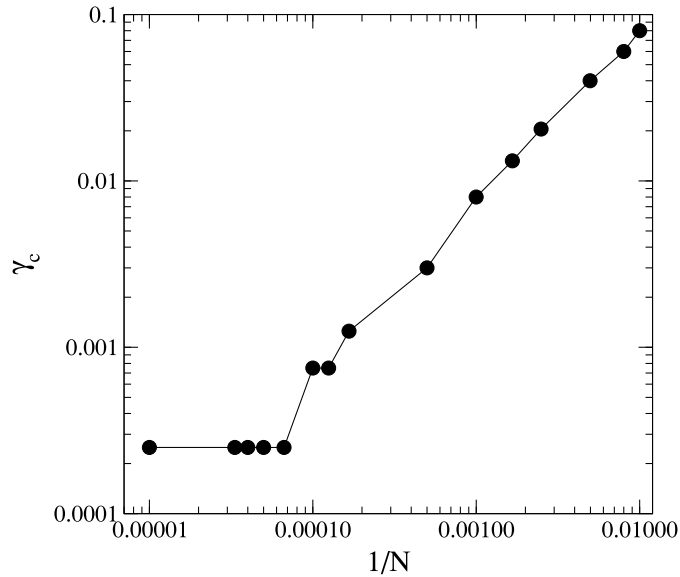


**Fig. 7.** Critical values of the inverse coupling length as a function of the inverse lattice size.

with its temporal average

$$\bar{R} = \lim_{T \rightarrow \infty} \frac{1}{T} \int_0^T R(t) dt. \tag{27}$$

The dependence of  $\bar{R}$  with the inverse coupling length  $\gamma$  is depicted in Fig. 6 for a fixed value of the coupling strength ( $K = 7$ ). For  $\gamma$  near zero we have a completely phase-synchronized state, as expected and, as  $\gamma$  varies through a critical value  $\gamma_c$  there is a transition to a non-synchronized state, which is observed for different values of  $N$ . The value of  $\gamma_c$  decreases as the lattice size increases. In Fig. 7 we plot the value of  $\gamma_c$  versus  $1/N$ . For relatively small chains  $\gamma_c$  decreases with  $1/N$  as a power-law with slope near the unity. As  $N$  increases further, the value of  $\gamma_c$  saturates at some value, namely 0.00025 at the thermodynamic limit.

On comparing Fig. 3 (frequency synchronization degree) and Fig. 6 (order parameter magnitude) one can see that the critical values of  $\gamma$  for frequency synchronization are always smaller than those for phase synchronization, considering the same lattice size. For example, for  $N = 2001$  oscillators  $\gamma_c \approx 0.003$  for frequency synchronization and  $\gamma_c = 0.005$

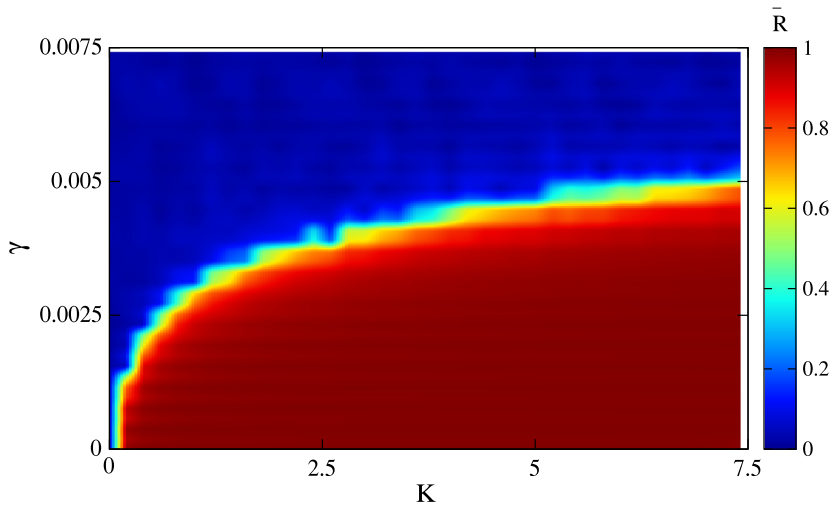


**Fig. 8.** (Color online) Order parameter magnitude (time-averaged) versus coupling parameters coupling strength  $K$  and inverse coupling length  $\gamma$  for a chain of  $N = 2001$  Kuramoto oscillators.

for phase synchronization. There results that, for  $0.003 < \gamma < 0.005$  we have frequency synchronization but no phase synchronization, in complete agreement with our previous observations.

Except for this differences, however, the general behavior of phase synchronization follows the same trends as frequency synchronization, as illustrated by Fig. 8, where we plot the time-averaged order parameter magnitude as a function of the coupling strength  $K$  and the inverse coupling length  $\gamma$ . We identify three regions in the diagram for which the dynamics is qualitatively different: in the deep blue region in Fig. 8 we have no phase synchronization, whereas in the red region complete phase synchronization is clearly seen. In between those regions there is a transitional regimes where the oscillator chain is partially phase synchronized.

## 5. Recurrence-based characterization

The characterization of spatial patterns can be also made by the introduction of recurrence-based quantification. It is well-known that time series of physical processes can be analyzed using recurrence plots, so as to unveil dynamical transitions and other features of the underlying dynamical system [18,19]. In this case a recurrence occurs when the state of the system approaches a previous value within some specified radius. We have extended this idea so as to interpret a spatial pattern (at fixed time) as a kind of “time series”, in which the role of time is played by the spatial separation  $j$  along the array of cells. For spatial patterns in which we discretize the points, as in a lattice, we say that two points apart from an integer distance  $j$  are recurrent if they have the same “height” up to some difference [20]. This analogy enables us to use the tools of recurrence quantification analysis to characterize complex patterns just like the ones we see in coupled oscillators [21,22].

We formally define a spatial recurrence matrix  $R_{ij}$  as follows. Consider a one-dimensional spatial pattern with  $N$  sites:  $\{x_k\}_{k=0}^N$  (just as the case of coupled oscillators) where two sites  $i$  and  $j$  have the same height, up to some precision  $\varepsilon$ , or  $|x_i - x_j| \leq \varepsilon$ . We say that, in a  $N \times N$  matrix the element  $R_{ij} = 1$ , otherwise (if the cells do not have the same values) it is  $R_{ij} = 0$ . In other words

$$R_{ij} = \Theta(|x_i - x_j| - \varepsilon), \quad (28)$$

where  $\Theta$  is the Heaviside unit step function. The spatial recurrence plot is a graphical representations of the spatial recurrence matrix with elements  $R_{ij}$ .

Each site is trivially recurrent to itself, such that  $R_{ii} = 1$  (usually these elements are removed from recurrence-based quantifiers). Moreover, the recurrence matrix is symmetric:  $R_{ji} = R_{ij}$ . The elements of the recurrence matrix depend on the radius of convergence  $\varepsilon$ : if the latter is too large all elements will be equal to the unity, whereas if  $\varepsilon$  is too small no recurrences would be detected. A convenient choice of  $\varepsilon$  is based on some fraction, say 10% of the mean square deviation of the heights for the spatial pattern. Other methods fix not  $\varepsilon$  itself but rather the recurrence-rate, which we define below.

A representative example of how much can recurrence plots contribute to the characterization of patterns in coupled oscillator chains is provided by Fig. 9, where we plot the spatial patterns for the phases and frequencies at fixed time and the corresponding spatial recurrence plots, for a chain of  $N = 401$  oscillators with  $K = 7.0$  and two values of  $\gamma$ . For  $\gamma = 0.023$  the phase pattern is poorly synchronized, and the recurrence plot displays mainly isolated points with a few horizontal structures [Fig. 9(a)]. On the other hand, the frequency pattern has a number of synchronization plateaus corresponding, in the recurrence plot, to highly recurrent black regions [Fig. 9(b)]. On slightly increasing the value of  $\gamma$  the phases are even less synchronized, presenting only isolated points which correspond to chance recurrences [Fig. 9(c)]. The frequencies,

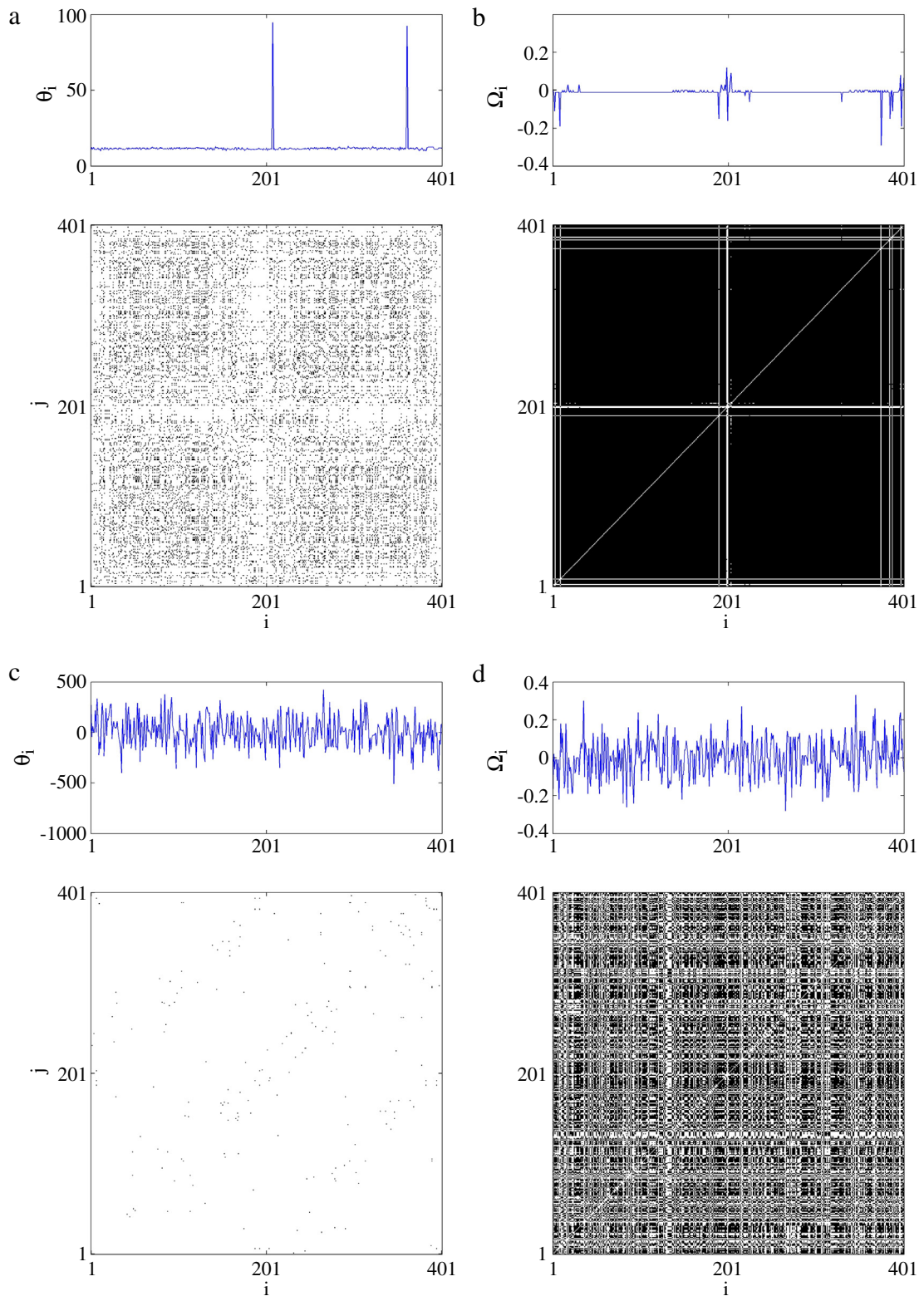


**Fig. 9.** (Color online) Spatial pattern for the (a) phases and (b) frequencies at time  $t = 15000$  and corresponding spatial recurrence plots for a chain of  $N = 401$  oscillators with  $K = 7.0$  and  $\gamma = 0.023$ . (c) and (d) are the corresponding figures for  $\gamma = 0.026$ .

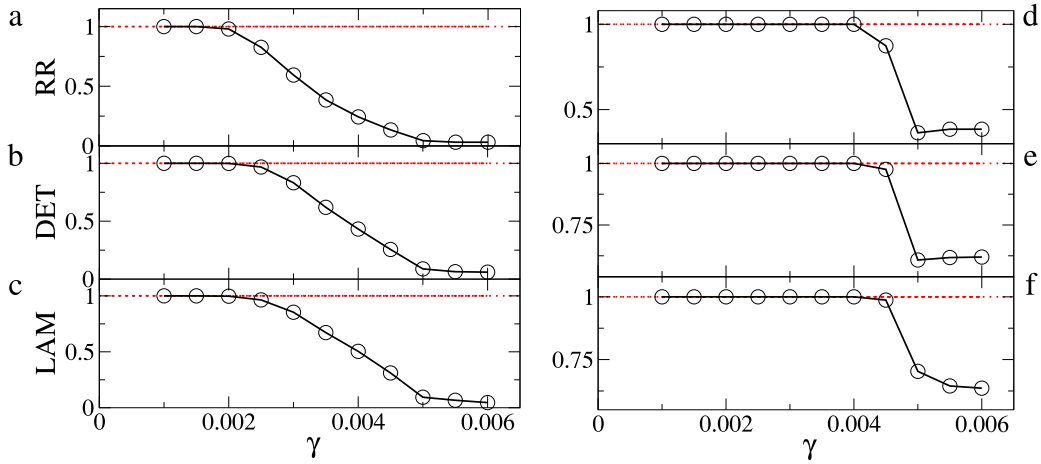


**Fig. 10.** (a) Recurrence rate, (b) determinism, and (c) laminarity as a function of the range parameter  $\gamma$  for the phases of  $N = 2001$  Kuramoto oscillators with  $K = 7.0$ . (d), (e) and (f) are the same but for the frequencies of the oscillators.

however, are more synchronized than the phases, what cannot be seen in the spatial pattern but can be inferred from the corresponding spatial recurrence plot [Fig. 9(d)].

There are many recurrence-based quantitative diagnostics available in the literature [19,23]. We found that three are enough to our purposes: the first is the recurrence rate ( $RR$ ), which is the fraction of recurrent points or the nonzero elements in the recurrence matrix:

$$RR = \frac{1}{N^2} \sum_{i=1}^N \sum_{j=1, j \neq i}^N R_{ij}. \quad (29)$$

The higher is  $RR$ , more recurrences occur. However, since recurrence points can occur by pure chance, we need other quantifiers, like the so-called determinism ( $DET$ ) (a term borrowed from the time-series analysis). The latter is the fraction of points in the spatial recurrence plots belonging to diagonal structures. For time series these diagonals occur due to deterministic evolution. On the other hand, in spatial patterns  $DET$  characterizes recurrent structures which cannot occur by pure chance.

We compute  $DET$  by taking  $\ell_{\min} = 2$  as the minimum length of a diagonal in the spatial recurrence plot, and searching all diagonal structures with different lengths  $\ell$ . Then we make a histogram, which is a numerical approximation of the probability distribution function  $P(\ell)$  of these lengths. The determinism is defined as the fraction of points in spatial recurrence plots belonging to diagonal structures:

$$DET = \frac{\sum_{\ell=\ell_{\min}}^N \ell P(\ell)}{\sum_{i, j \neq i} R_{ij}}. \quad (30)$$

Accordingly, in a completely disordered pattern there would be no diagonal structures, and  $DET$  would be near zero.

There are also horizontal structures in the recurrence plots (equivalent to vertical structures due to symmetry), which are also helpful to distinguish true recurrences from chance recurrences. Moreover such horizontal structures are directly related to plateaus in the corresponding spatial patterns. The quantifier, in this case, is aptly called laminarity ( $LAM$ ), which we compute by counting how much horizontal structures of length  $\nu > \nu_{\min} = 2$  exist in the spatial recurrence plot, what gives us and another probability distribution function  $P(\nu)$ , from which we have

$$LAM = \frac{\sum_{\nu=\nu_{\min}}^N \nu P(\nu)}{\sum_{\ell=1}^N \nu P(\nu)}. \quad (31)$$

We begin our analysis by considering the three regimes observed in the parameter space depicted in Figs. 8 and 4, for phase and frequency synchronization, respectively. Let us consider a fixed value of  $K$ , say 7.0 and consider the increase of the value of  $\gamma$ . In Fig. 10 we plot the values of recurrence rate, determinism and laminarity of spatial recurrence plots obtained for increasing values of  $\gamma$  from the phase and spatial patterns with  $N = 2001$  oscillators. The values represent averages over

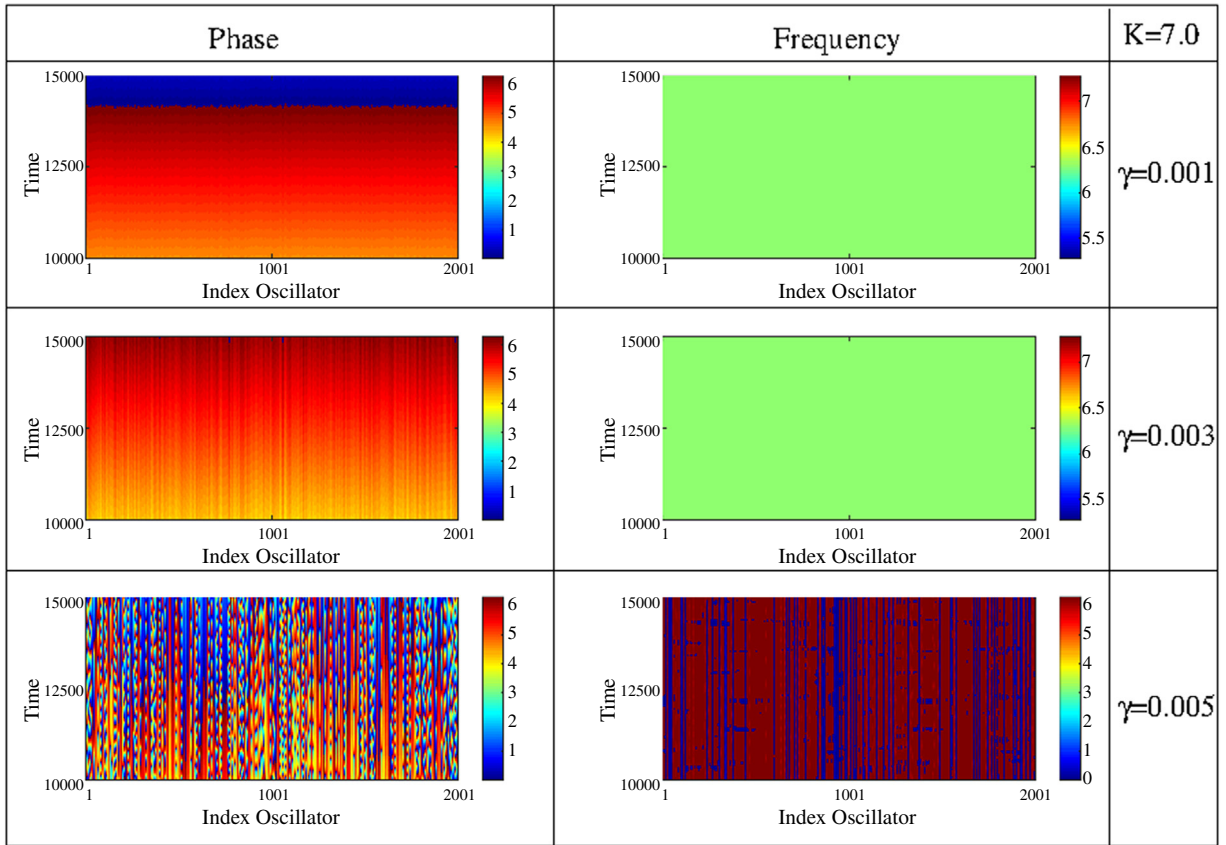


**Fig. 11.** (Color online) Spacetime plots for the oscillator phases in the case  $K = 7.0$  and (a)  $\gamma = 0.001$ , (b)  $0.003$ , (c)  $0.005$ . (d), (e), and (f) are spacetime plots for the oscillator frequencies and the same values of  $\gamma$  as (a), (b) and (c), respectively.

$5 \times 10^3$  time units, discarding the first  $10^4$  transients. The radius of recurrence was chosen as being 10% of the mean square deviation.

The recurrence rate decreases as  $\gamma$  increases, showing that the phases start losing complete synchronization at  $\gamma \approx 0.002$  and become totally non-synchronized at  $\gamma \approx 0.005$  [Fig. 10(a)]. These findings are confirmed by the determinism and laminarity [Fig. 10(b) and (c), respectively]. In addition, in Fig. 11(a), (b) and (c) we show spacetime plots showing the phase evolution for a totally synchronized, partially synchronized and non-synchronized cases, respectively.

A similar analysis can be made on the spatial pattern obtained from the frequencies of the coupled oscillators. The *RR* decreases with  $\gamma$  but in this case the transition starts later than for the phases. For example the *RR* starts to decrease at  $\gamma \approx 0.004$  [Fig. 10(d)], whereas the *RR* for the phases does so much earlier, at  $\gamma \approx 0.002$ . This is due to the well-known fact that oscillators can have different phases but same frequencies, hence frequency synchronization is more difficult to break than phase synchronization. The critical value of  $0.002$  was observed to be the same for two convergence radius. This behavior is followed by *DET* and *LAM* [Fig. 10(e) and (f), resp.].

## 6. Conclusions

Some of the results we obtained on phase synchronization can be interpreted in the light of the mathematical treatment (mean field theory) available for the Kuramoto model with global (all-to-all) coupling, which corresponds to the  $\gamma \rightarrow 0$  limit of our theory. The uncoupled oscillators are supposed to have randomly distributed frequencies and phases, the former according to a specified probability distribution function  $g(\omega)$  such that there is a single maximum at  $\omega = 0$  and the PDF is symmetric with respect to this value ( $g(-\omega) = g(\omega)$ ).

In this case of global coupling, using the order parameter defined in (26) the oscillator chain can be written in the following form

$$\dot{\theta}_j = \omega_j + KR \sin(\Psi - \theta_j), \quad (32)$$

where we can set  $\Psi = 0$  by transforming to a rotating frame.

It is well-known that, for weak coupling (corresponding to small values of the coupling constant  $K$ ), the oscillators remain non-synchronized (in both phase and frequency) since the coupling effect is too weak to overcome the natural disorder of

the oscillator frequencies characterized by  $g(\omega)$ . However, even if  $K$  is very small, it turns out that some of the oscillators synchronize their phases, namely those with natural frequencies near zero. In particular, if  $-KR \leq \omega_j \leq KR$  the oscillators are synchronized in frequency since they are all stationary in the rotating frame. Such oscillators are not phase-synchronized though, for their phases are given by  $\sin \theta_j = \omega_j / KR$ . The oscillators with natural frequencies  $|\omega_j| > KR$  will not synchronize their frequencies. They are often called drifting oscillators, whereas the synchronized ones are also called locked oscillators.

As  $K$  increases, the fraction of drifting oscillators decreases and the chain becomes partially phase and frequency synchronized. It is worthwhile to note that two or more oscillators can be frequency synchronized without phase synchronization. For a given value of  $K$  the degree of frequency synchronization is expected to be always higher than the degree of phase synchronization. As a matter of fact, complete phase synchronization would be achieved only in the limit of very large  $K$ .

Another familiar aspect of the classical Kuramoto model (32) is the existence of a structural phase transition from non-synchronized to partial synchronization as  $K$  increases past a critical value  $K_c$ . A mean-field analysis shows that  $K_c = 2/\pi g(0)$  and the order parameter magnitude, just after  $K_c$ , grows quadratically like  $(K - K_c)^{1/2}$ .

Those features have been reproduced, in our chemically coupled Kuramoto oscillators, for  $\gamma = 0$ . Moreover, by continuity, we expect that such features continue to be present for  $\gamma$  small but nonzero. On the other hand, as  $\gamma$  increases further, the coupling becomes more of a local type and thus the mean-field analysis fails. Physically we can say that the diffusion effect due to the coupling may not be enough to overcome the natural disorder of the oscillators. Indeed, for large  $\gamma$  (local coupling) there is no frequency or phase synchronization at all, even for large  $K$ .

The loss of synchronizability is revealed by the fact that a synchronization transition also exist if we vary the effective range  $\gamma$  for fixed  $K$ : a synchronized chain for small  $\gamma$  can become non-synchronized as  $\gamma$  increases past a critical value  $\gamma_c$ . Our results have indicated that, while the phase synchronization occurs gradually as a parameter is varied, the frequency synchronization is more abrupt. This difference between the transitions is due to the exponential decay of the interaction strength with the lattice distance, that is related to a diffusion process for the chemical which mediates the coupling among oscillators.

## Acknowledgments

This work was made possible with the help of CNPq (grant nos. 303888/2014-8 and 441553/2014-1), CAPES, FAPESP, and Fundação Araucária (Brazilian Government Agencies).

## References

- [1] J.D. Murray, *Mathematical Biology. Vol. II: Spatial Models and Biomedical Applications*, third ed., Springer Verlag, New York-Berlin-Heidelberg, 2003.
- [2] Y. Kuramoto, *Progr. Theoret. Phys.* 94 (1995) 321.
- [3] Y. Kuramoto, H. Nakao, *Phys. Rev. Lett.* 76 (1996) 4352.
- [4] Y. Kuramoto, H. Nakao, *Physica D* 103 (1997) 294.
- [5] D. Battogtokh, *Progr. Theoret. Phys.* 102 (1999) 947.
- [6] H. Nakao, *Chaos* 9 (1999) 902.
- [7] Y. Kawamura, N. Nakao, Y. Kuramoto, *Phys. Rev. E* 75 (2007) 036209.
- [8] D. Battogtokh, *Phys. Lett. A* 299 (2002) 558.
- [9] H. Sakaguchi, *Phys. Rev. E* 73 (2006) 031907.
- [10] A.M. Batista, S.E. de S. Pinto, R.L. Viana, S.R. Lopes, *Phys. Rev. E* 65 (2002) 056209.
- [11] C. Anteneodo, S.E. de S. Pinto, A.M. Batista, R.L. Viana, *Phys. Rev. E* 68 (2003) 045202.
- [12] R.L. Viana, C. Grebogi, S.E. de S. Pinto, S.R. Lopes, A.M. Batista, J. Kurths, *Physica D* 206 (2005) 94.
- [13] Y. Kuramoto, in: H. Araki (Ed.), *Lecture Notes in Physics*, in: *International Symposium on Mathematical Problems in Theoretical Physics*, vol. 39, Springer-Verlag, New York, 1975, p. 420.
- [14] Y. Kuramoto, *Chemical Oscillations, Waves, and Turbulence*, Springer-Verlag, New York, 1984.
- [15] S. Strogatz, *Physica D* 143 (2000) 1.
- [16] J.A. Acebrón, L.L. Bonilla, P. Vicente, J. Conrad, F. Ritort, R. Spigler, *Rev. Modern Phys.* 77 (2005) 137.
- [17] D.B. Vasconcelos, R.L. Viana, S.R. Lopes, A.M. Batista, S.E. de S. Pinto, *Physica A* 343 (2004) 201.
- [18] J.P. Eckmann, S.O. Kamphorst, D. Ruelle, *Europhys. Lett.* 4 (1987) 963.
- [19] N. Marwan, M.C. Romano, M. Thiel, J. Kurths, *Phys. Rep.* 438 (2007) 237.
- [20] D.B. Vasconcelos, R.L. Viana, S.R. Lopes, J. Kurths, *Phys. Rev. E* 73 (2006) 056207.
- [21] F.A. dos S. Silva, S.R. Lopes, R.L. Viana, *Commun. Nonlinear Sci. Numer. Simul.* 35 (2016) 37.
- [22] M.S. Santos, J.D. Szezech Jr., A.M. Batista, I.L. Caldas, R.L. Viana, S.R. Lopes, *Phys. Lett. A* 379 (2015) 2188.
- [23] J.P. Zbilut, C.L. Webber Jr., *Phys. Lett. A* 171 (1992) 199.